The Measurement of Rotational Relaxation Time T_2 for $CH_3C^{15}N$ Self- and Foreign Gas Collisions

H. Mäder, H. Bomsdorf and U. Andresen

Abteilung Chemische Physik im Institut für Physikalische Chemie der Universität Kiel

Z. Naturforsch. **34a**, 850–857 (1979); received April 28, 1979

We report on the measurement of T_2 for several rotational transitions of $CH_3C^{15}N$. The transient emission signal is investigated at different temperatures for the pure gas and mixtures with He and H_2, and effective collision diameters are derived from the pressure dependence of T_2.

I. Introduction

Transient experiments in gas phase microwave spectroscopy have been developed in the past few years to investigate molecular rotational relaxation processes [1]. The information on bulk relaxation data obtained from these studies may be useful to understand molecular collision dynamics and thereby the intermolecular potential. Such information has also become important for elucidating the non-thermal rotational energy distribution of interstellar molecules.

Transient microwave experiments have predominantly been carried out on two-level quantum mechanical systems. The relaxation times T_1 and T_2 which describe phenomenologically the decay of population difference and induced polarisation to equilibrium, respectively, are obtained from such time-domain experiments.

We report here on the measurement of T_2 on several rotational transitions of an isotope of methyl cyanide, $CH_3C^{15}N$, by analysis of the transient emission signal. This time-resolved experimental technique is complementary to the more traditional line-width measurements which are complicated by the additional effects of power and modulation broadening. In addition, transient Stark-switching technique is easier to apply to the study of the M-dependence of relaxation times [2].

The theory describing the observed transient phenomena is briefly summarized in Section II. In Sect. III we report on the experimental setup and the results for the pressure and temperature dependence of T_2 for the pure gas and for mixtures with He and H_2.

Reprint requests to Dr. H. Mäder, Abt. Chemische Physik im Institut für Physikalische Chemie der Universität Kiel, Olshausenstr. 40/60, D-2300 Kiel.

0340-4811 / 79 / 0700-0850 $ 01.00/0

II. Theory

The basic Bloch-type equations which govern the interaction of coherent electromagnetic radiation with a quantum-mechanical system undergoing collisional relaxation are derived in detail elsewhere [3]. An extended treatment also valid in the case of non-vanishing diagonal dipole matrix elements has been given recently [4]. We present here only the results.

Within the rotating wave approximation *, the time dependence of the Fourier components, P_r and P_i, of the polarisation, together with the two-level population difference ΔN are determined by three coupled differential equations,

$$\begin{aligned} &\dot{P}_r + \Delta\omega\, P_i + \frac{P_r}{T_2} = 0\,, \\ &\dot{P}_i - \Delta\omega\, P_r + \frac{\hbar^2\varkappa^2}{4}\,\varepsilon\,\Delta N + \frac{P_i}{T_2} = 0\,, \\ &\frac{\hbar}{4}\,\dot{\Delta N} - \varepsilon\, P_i + \frac{\hbar}{4}\,\frac{\Delta N - \Delta N_0}{T_1} = 0\,, \end{aligned} \tag{1}$$

where ε is the electric field amplitude of the polarizing radiation. The relaxation of ΔN to its Boltzmann equilibrium value ΔN_0 is described by T_1, the relaxation time T_2 is a measure of the decay of polarization, P_r and P_i, to zero equilibrium. $\Delta\omega$ is the difference between molecular transition angular frequency ω_0 and the angular frequency ω of the radiation. $\varkappa$ is proportional to the transition electric dipole matrix element, $\varkappa = 2\,|\mu_{ab}|/\hbar$.

We are interested here in solutions of Eq. (1) which are applicable to the analysis of the transient emission signal to determine the relaxation time T_2.

* Neglection of high-frequency terms due to diagonal dipole matrix elements, as justified for the experimental conditions (see Sect. III), included.

Transient emission is observed when the system is brought from resonance with the coherent radiation into far-off resonance in times which are short with respect to the relaxation times. Experimentally such switching of the resonance condition may be performed by using the molecular Stark-effect to switch the molecular energy level difference as described in detail in the following section. The transient emission signal $\Delta S(t)$ which is observed at the output of a square law diode detector may be interpreted as the beat of the microwave radiation from the external source with the field emitted from the polarized molecular sample.

Neglecting the velocity distribution of molecules, we have [4]

$$\Delta S(t) = \frac{8\pi\beta\omega_0 L}{c}\left(\frac{\sin\frac{\Delta k L}{2}}{\frac{\Delta k L}{2}}\right)\varepsilon P_i(0)\, e^{-t/T_2}\cdot \cdot\cos\left(\Delta\omega t - \frac{\Delta k L}{2}\right). \quad (2)$$

$P_i(0)$ is the initial value of P_i at time $t=0$ when the system is switched out of resonance; L is the absorption cell length, β a constant characterizing the diode efficiency, and $\Delta k = \Delta\omega/c$ the change of wave vector k due to Stark-switching.

In order to account for the motion of molecules (Doppler-effect) one has to integrate Eq. (2) over the Maxwell velocity distribution along the direction of the wave propagation, replacing $\Delta\omega$ in Eq. (2) by the Doppler-shifted expression $\Delta\omega + \omega_0 v/c$. Then, in the pressure-broadened limit [3], we have

$$\Delta S(t) = A\, e^{-t/T_2} e^{-t^2/4q^2} \cos\Delta\omega\left(t - \frac{L}{2c}\right) \quad (3)$$

where

$$A = 8\pi\beta\frac{\omega_0}{c} L\varepsilon P_i(0),$$

$$q = \sqrt{\ln 2}/\Delta\omega_0$$

with the Doppler-width

$$\Delta\omega_0 = \frac{\omega_0}{c}\sqrt{\frac{2RT\ln 2}{M}}$$

which depends on the molecular transition frequency ω_0, the temperature T, and the molecular weight M.

When deriving Eq. (3), use has been made of the fact that

$$\Delta\omega_D \ll \frac{1}{T_2} + \frac{T_1}{T_2}\varkappa^2\varepsilon^2 \quad \text{and} \quad \Delta k L \ll 1$$

which holds for the experimental conditions (see Section III). Recently it has been shown from frequency domain considerations [5] that Eq. (3) applies also for propagating or standing waves in a waveguide. The resulting expression which is known as a Voigt profile represents the Fourier Transform of Eq. (3) in the low power limit [6].

III. Experimental and Results

The experimental arrangement which was used for the observation of the transient signals is schematically shown in Figure 1. The microwave radiation was supplied from phase stabilized BWO's and fed into a conventional Stark cell consisting of a rectangular waveguide (with inner dimensions 1×4.7 cm) and a tefloninsulated Stark septum. For the pressure measurements a MKS-Baratron 310 B capacitance manometer was used. In order to stabilize the pressure and minimize the influence of selective adsorption of the mixture components on the walls of the sample system we attached a 20 l bulb. To allow for temperature variation (room temperature to -70 °C) the cell was cooled with methanol flowing through a cooling jacket.

Different types of Stark generators have been used to supply the Stark field. For the $K=0$ transitions which exhibit quadratic Stark effect, we used a generator which produced pulses of variable length (0.3—3 μsec) and amplitude (<450 volt). For transitions with $|K|=1$ which, because of linear Stark effect, are very sensitive to variations of the Stark field amplitude, the pulses were supplied by a commercial generator (Anritsu MG 412 A). The microwave radiation was detected by means of 1N26 (Ku-band) and 1N53 (V-band) crystals. A potentiometer (0—1 kΩ) to shunt the crystal current to ground was used to optimize the crystal sensitivity. The signal was then amplified by two broadband amplifiers (Avantek GDP 601—603, 200 Hz to 400 MHz, 36 db; PAR Mod. 115, DC-70 MHz, 20 db or 40 db) and then fed into a Boxcar integrator (PAR Mod. 162/164). Further averaging for repeated experiments was obtained by A/D converting the Boxcar output signal and using a digital aver-

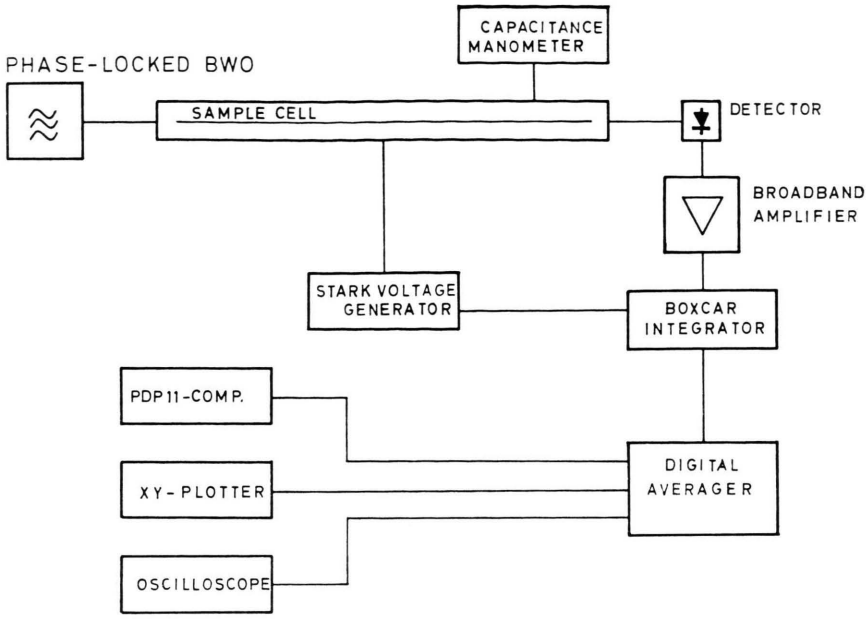

Fig. 1. Schematic block diagram of the experimental arrangement.

ager (Fabri-Tek Mod. 1072). Its memory contents could be displayed on a X-Y-plotter or an oscilloscope.

For further analysis of the transient signal the data were transferred to a PDP-11 computer. Due to the fact that the computer was about 50 m apart, the binary data were converted to BCD code and then transmitted bit parallel/data seriell. The controlling computer program takes care of the large voltage swing on the transmission line by waiting until the output is stable.

The programm also converts the incoming BCD data to the internal real number representation and makes them available to the analysis program.

The sample gas consisted of 95% $CH_3C^{15}N$ and 5% $CH_3C^{14}N$. No impurities which could influence the results were found from a gas chromatogram. The sample pressure was varied from about 1 to 20 mTorr for the pure gas. The partial pressures for the foreign gases (He, H_2) were in the range of 0 to 150 mTorr. The method to determine the partial pressures and check the reliability of the mixing procedure has been described in detail elsewhere [7].

For the pure gas, we measured at room temperature the pressure dependence of $1/T_2$ for the transitions (J, K, M):

$$(0, 0, 0)\text{–}(1, 0, 0)^*, \quad (1, 0, 0)\text{–}(2, 0, 0),$$
$$(1, \pm 1, \pm 1)\text{–}(2, \pm 1, \pm 1) \quad \text{and}$$
$$(1, \pm 1, \mp 1)\text{–}(2, \pm 1, \mp 1)$$

in the ground vibrational state and the transitions (J, K, M, l):

$$(1, \pm 1, \pm 1, \pm 1^1)\text{–}(2, \pm 1, \pm 1, \pm 1^1)^{**},$$
$$(1, \pm 1, \pm 1, \pm 1^2)\text{–}(2, \pm 1, \pm 1, \pm 1^2)^{**}$$

and

$$(1, \pm 1, \pm 1, \pm 1)\text{–}(2, \pm 1, \pm 1, \mp 1)$$

in the first excited CCN-bend vibrational state ($v_8 = 1$). The investigation was extended to temperatures 0 °C, −25 °C, and −50 °C for the ground state (0, 0, 0)–(1, 0, 0) and (1, ±1, ±1)–(2, ±1, ±1) transitions. The results are given in Table I.

To demonstrate the observed signal behaviour, the transient absorption ($\pi/2$-pulse)-emission signal is shown for the (1, 0, 0)–(2, 0, 0) transition at two different pressures in Figure 2. The Stark pulse which brings the molecules into resonance with the microwaves is relatively short (~ 300 nsec) due to the large transition dipole moment of CH_3CN. For the same reason, to minimize the influence of far-off resonant absorption in the transient emission period, the frequency offset has been chosen to be relatively high (beat frequency ~ 8 MHz).

* For the investigation of the transient emission signal of this transition the Boxcar integrator was replaced by a transient digitizer (Biomation Mod. 6500).

** The index $l^{1,2}$ is used to distinguish between the two components of the $l = \pm 1$ transition [8].

Table 1. Slope (β) and intercept (α) from the least squares analysis of the plots of $1/T_2$ against pressure of $CH_3C^{15}N$. The values in parantheses result from an approximative correction for interfering local electric fields, see text. The given errors ($\Delta\alpha$, $\Delta\beta$) are the standard deviations.

Transition	Polarized M-component	T [K]	β [μsec^{-1} mTorr^{-1}]	$\Delta\beta$ [μsec^{-1} mTorr^{-1}]	α [μsec^{-1}]	$\Delta\alpha$ [μsec^{-1}]
$J=1-2,\ K=\pm 1$	$M=\mp 1$	299	0.354 (0.382)	0.002	0.629 (0.04)	0.014
$J=1-2,\ K=\pm 1$	$M=\pm 1$	298	0.357 (0.388)	0.001	0.585 (0.04)	0.007
		273	0.376 (0.409)	0.003	0.548 (0.04)	0.016
		248	0.408 (0.445)	0.002	0.628 (0.04)	0.009
		223	0.443 (0.482)	0.002	0.583 (0.04)	0.009
$J=1-2,\ K=0$	$M=0$	299	0.388	0.002	0.086	0.007
$J=0-1,\ K=0$	$M=0$	296	0.463	0.002	0.009	0.010
		273	0.501	0.002	−0.005	0.008
		247	0.534	0.004	−0.033	0.013
		222	0.568	0.004	−0.028	0.014
$\nu_8=1\left(\begin{smallmatrix}J=1-2\\K=\pm 1,l=\pm 1^1\end{smallmatrix}\right)$	$M=\pm 1$	296	0.439	0.002	−0.021	0.007
$\nu_8=1\left(\begin{smallmatrix}J=1-2\\K=\pm 1,l=\pm 1^2\end{smallmatrix}\right)$	$M=\pm 1$	298	0.430	0.002	0.033	0.006
$\nu_8=1\left(\begin{smallmatrix}J=1-2\\K=\pm 1,l=\mp 1\end{smallmatrix}\right)$	$M=\pm 1$	296	0.356 (0.389)	0.003	0.672 (0.04)	0.015

To switch the (1, 0, 0)–(2, 0, 0) transition from resonance into far-off resonance with the microwave radiation without polarizing other transitions, we had to switch the Stark voltage from 230 V to 25 V instead of to zero volt as usually done in this type of experiment. The necessity of such a Stark field offset may be explained by means of Fig. 3 which schematically shows the frequency pattern of the $J=1-2$, $K=0, \pm 1$ transitions for different Stark voltages. When switching from high Stark field (c) to zero field (a) and vice versa, the $K=\pm 1$, $M=\pm 1$ component is polarized by fast passage [9] and emits at the frequency of the $K=\pm 1$ component which appreciably disturbs the emission signal under consideration. As seen from Fig. 3 this problem is circumvented by switching from (c) to the small Stark field (b) where the $K=0$, $M=0$ transition is shifted about 80 kHz from zero field frequency. The transient emission of this transition now takes place in the presence of a small electric field, which is slightly inhomogeneous according to the type of Stark cell used in the experiment. Such field inhomogeneity gives rise to an additional dephasing of the coherently prepared molecules and thus leads to a faster T_2-decay. In order to estimate the magnitude of this effect, we have also investigated the transient emission signal for two other offset voltages (35 V and 45 V). Within the given uncertainties of the pressure dependence of $1/T_2$ as discussed later in this section, we found no significant variation of the results which are given in Table I for the measurements with 25 V Stark offset.

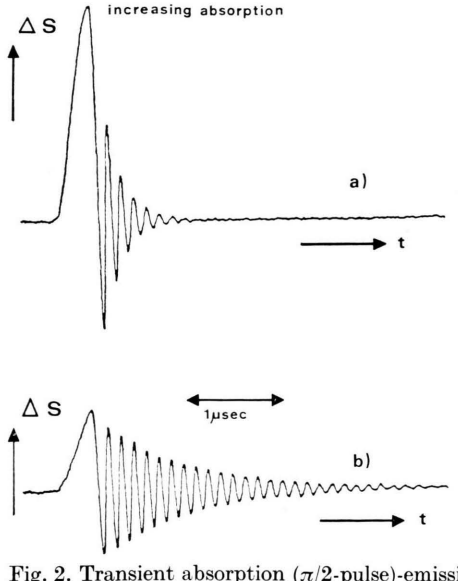

Fig. 2. Transient absorption ($\pi/2$-pulse)-emission signal for the J, K, M: (1, 0, 0)–(2, 0, 0)-transition of $CH_3C^{15}N$ at room temperature. a) $p = 13$ mTorr, b) $p = 3$ mTorr.

The analysis of the data was performed by least square fitting the expression

$$S(x) = A\, e^{-Bx}\, e^{-x^2/4q^2} \cdot \cos(Cx + D) + Ex + Fx^2 + G \quad (4)$$

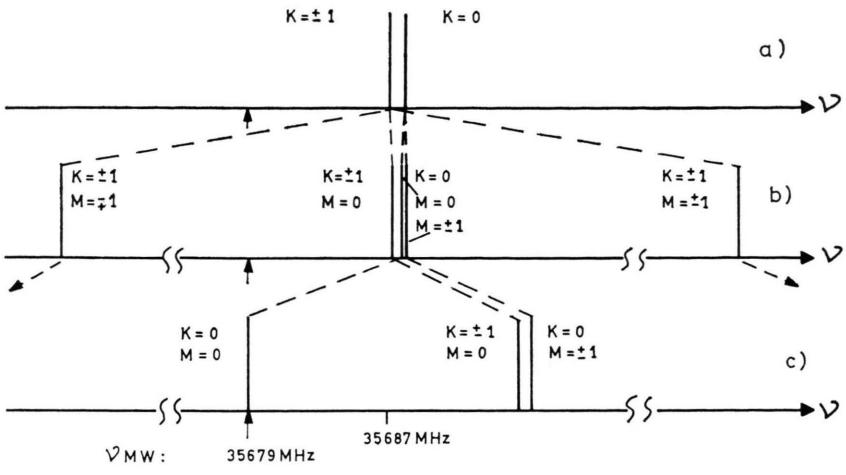

Fig. 3. Transition frequency pattern for the $J = 1 - 2$, $K = 0, \pm 1$ transitions. a) $U_{stark} = 0$ V, b) $U_{stark} = 25$ V, c) $U_{stark} = 230$ V. Microwave frequency fixed at 35679 MHz. Position of the $K = \pm 1$ lines (b) is not on scale.

to the data points stored in the PDP 11 computer, with the constants A to G as fitting parameters*. The linear relation between data point interval Δx and time was obtained by comparison with a 5 MHz sinusoidal calibration signal. The terms $Ex + Fx^2$ account for a small time-dependent distortion of the signal due to the bandwidth limitation of the detection circuits, G stands for an arbitrary DC offset of the signal. Besides these terms Eq. (4) corresponds to the theoretical expression for $\Delta S(t)$, Eq. (3), and the inverse relaxation time $1/T_2$ is obtained together with its standard error from the least squares procedure once the time calibration is known. From the results at different sample pressures the coefficients of the linear pressure dependence are then evaluated by using a linear least squares fit and weighting the $1/T_2$ data points with their standard deviations.

The standard errors of the results for the intercept (α) and slope (β) which are given in Table I do not reflect systematic deviations which are primarily due to shifts in pressure (< 0.1 mTorr) and temperature (< 1 °C). These inaccuracies of the experimental conditions lead to an additional error for the slope ($\sim 3 \cdot 10^{-3}$ μsec^{-1} mTorr^{-1}) and the intercept ($\sim 4 \cdot 10^{-2}$ μsec^{-1}). The intercept is caused by collisions of molecules with the walls of the sample cell. This wall collision contribution to $1/T_2$ may be estimated to be approximately $4 \cdot 10^{-2}$ μsec^{-1} by using simple kinetic arguments [5]. For the ground state $K = 0$ transitions and the $v_8 = 1$, M, $l = \pm 1$, $\pm 1^{1,2}$ transition, with quadratic Stark effect for small fields, this value is within the estimated inaccuracies in accordance with our results (see, for example, Figure 4).

The intercept values which were obtained for the lines with linear Stark effect are larger than expected, see Table I. In contrast to the lines with quadratic Stark effect (see discussion above), these lines would already be affected in width ($\sim 1/T_2$) for small offsets from a zero Stark field. Thus, for example a 10% increase of $1/T_2$ results from an offset voltage of 0.2 V for the

$$(J, K, M): (1, \pm 1, \pm 1) - (2, \pm 1, \pm 1)$$

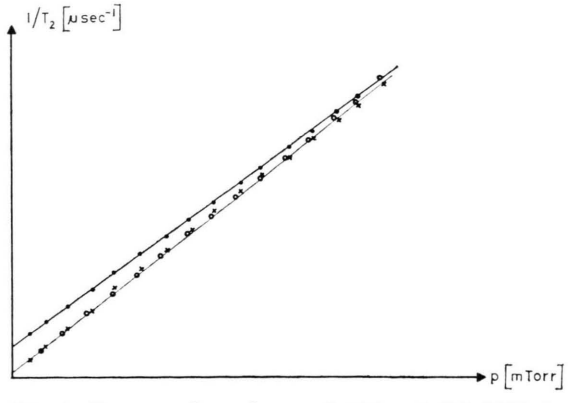

Fig. 4. Pressure dependence of $1/T_2$ of $CH_3C^{15}N$ from transient emission. Data points for the (J, K, M): $(1, \pm 1, \pm 1)$-$(2, \pm 1, \pm 1)$ transition are denoted by ●, the corrected points by × and the results for the (J, K, M): $(1, 0, 0)$-$(2, 0, 0)$ transition by ○. The fitted straight lines for the latter two sets of points coincide approximately.

* The term $\exp(-x^2/4q^2)$ was held fixed and calculated from Doppler-broadening, correcting for transitions with linear Stark effect see below and appendix.

Table 2. Slopes (γ) from the least squares analysis of the plots of $1/T_2$ against pressure of He and H_2. The given errors ($\Delta\gamma$) are the standard deviations.

Transition	Polarized M-component	T [K]	p_{CH_3CN} [mTorr]	γ [μsec^{-1} mTorr^{-1}]	$\Delta\gamma$ [μsec^{-1} mTorr^{-1}]
CH_3CN-He					
$J=1-2$, $K=\pm1$	$M=\pm1$	297	3.0	0.0226	0.0001
		297	5.0	0.0228	0.0001
$J=1-2$, $K=0$	$M=0$	297	5.0	0.0202	0.0002
$J=0-1$, $K=0$	$M=0$	293	5.0	0.0215	0.0002
CH_3CN-H_2					
$J=1-2$, $K=\pm1$	$M=\pm1$	295	3.0	0.0488	0.0004
		296	5.0	0.0488	0.0003
$J=1-2$, $K=0$	$M=0$	299	5.0	0.0467	0.0003
$J=0-1$, $K=0$	$M=0$	294	4.8	0.0509	0.0006

transition at 1.7 mTorr. However, the Stark baseline could be adjusted well enough to zero (accuracy 0.02 V) such that the apparent intercept discrepancy cannot be explained by a residual electric field which is produced by the Stark generator.

It seems reasonable to assume that the presence of static electric charges, most probably located on the teflon insulation of the Stark septum, gives rise to small electric field components which cause spatial incoherence and thus affect the T_2-relaxation. It is difficult to account for this effect quantitatively as the magnitude of these electric fields at different points of the sample cell is not known. To get an estimate of its influence on the determination of the pressure dependence of $1/T_2$, we have made the assumption that the frequency shifts which are induced by such local fields are normal distributed with the respect to zero field molecular transition frequency. Then, as shown in the appendix, the resulting transient emission signal may be given analytically by Eq. (3) where the "Doppler-correction" constant $\tilde{q}$ is not only determined by the velocity distribution of molecules but also by the interfering fields. By adjusting this constant empirically** such that the intercept for the pressure dependence of $1/T_2$ agrees with the estimate of 0.04 μsec^{-1}, the resulting slope will also be affected. As an example, Fig. 4 shows the measured $1/T_2$ values at different pressures together with the corrected points for the

$$(J, K, M): (1, \pm1, \pm1) - (2, \pm1, \pm1)$$

transition at room temperature. Though less accurately determined, the corrected slope values (see Table I) are thought to be a better approach to the T_2-relaxation on account of molecular collisions.

For the mixtures the dependence of $1/T_2$ on the partial pressure is linear in the binary collision approximation, $1/T_2 = \alpha + \beta p_{CH_3CN} + \gamma p_{He(H_2)}$. The coefficients γ were obtained from a linear least squares fit and are given in Table II. The independence of the CH_3CN partial pressure is demonstrated for the $K=\pm1$ line. Systematic deviations which arise from pressure and temperature shifts, partial pressure inaccuracies and electretic fields (for the $K=\pm1$ line***) are not covered by the given standard deviation and are estimated to be approximately 5%.

IV. Discussion

As seen from the results in Table I the T_2-relaxation for the pure gas is significantly faster for the ground state $J=0-1$ transition as compared to the $J=1-2$ transition. The same tendency has been obtained from linewidth studies for the normal species $CH_3C^{14}N$, carried out by Story et al. [10], Srivastava et al. [11], and Roberts et al. [12]. The

** The factor $\tilde{q}$ had to be chosen to be approximately a quarter of the value from Doppler-contribution, corresponding to a field distribution of about 100 mV/cm (HWHM) with respect to zero field.

*** Compared to the pure gas, the local interfering fields were found to be less effective in shifting the smaller pressure coefficients for the mixtures.

Table 3. Pressure broadening parameters $\Delta\nu_p^{exp}$ as obtained from linewidth studies for $CH_3C^{14}N$ and from transient emission investigation ($\Delta\nu_p = \beta/2\pi$) for $CH_3C^{15}N$. The calculated values $\Delta\nu_p^{calc}$ were obtained by means of the Murphy-Boggs (MB) and Anderson-Tsao-Curnutte (ATC) theory, for details and references see Refs. [11, 12].

Ref.	$CH_3C^{14}N$ Transition	$\Delta\nu_p^{exp}$ [MHz · mTorr^{-1}]	$\Delta\nu_p^{calc}$ [MHz · mTorr^{-1}] MB	ATC	$CH_3C^{15}N$ Transition	$\Delta\nu_p^{exp}$ [MHz · mTorr^{-1}]
[10]	$J = 1 - 2$, $K = 0$	0.0412 [b]	—	—	$J = 1 - 2$, $K = 0$	0.0617 [a]
[11]	$F = \binom{1-2}{2-3}$	0.0406 [a]	0.0701	0.0828		
[12]	$J = 0 - 1$, $K = 0$ $F = 1 - 2$	0.0942 [b]	—	0.0917	$J = 0 - 1$, $K = 0$	0.0736 [a]

[a] Measurements taken at room temperature. [b] No temperature given.

pressure broadening parameters $\Delta\nu_p$, as obtained by these authors, are given in Table III together with our results for the corresponding transition of the isotopic species. The apparent discrepancy of the experimental results for the two species is thought to be primarily due to the interfering quadrupole hyperfine structure of the $CH_3C^{14}N$ lines which does not exist for the isotopic species and which has not been considered explicitely in the line-width studies. In addition, for the $J = 1 - 2$, $K = 0$ transition, no line shape correction has been carried out to account for the overlapping $K = \pm 1$ line which is only 0.5 MHz apart. In our study, this interfering effect is circumvented by the Stark-switching technique; see discussion in Section III. The results from theoretical linewidth calculations, also given in Table III, confirm the J-dependence behaviour and are in better accordance with our measurements.

It is possible to describe the temperature dependence of T_2 by comparing the results of the measurements at temperature T with those at room temperature ($\sim 300\,^\circ$K) [13]:

$$\frac{(1/T_2)_T}{(1/T_2)_{300}} = \left(\frac{T}{300}\right)^{\varrho} . \tag{5}$$

The coefficient ϱ was derived from a least squares procedure to be

$$\varrho = -0.76 \pm 0.03$$

for the $J = 1 - 2$, $K = \pm 1$ transition, and

$$\varrho = -0.70 \pm 0.06$$

for the $J = 0 - 1$, $K = 0$ transition. These values are close in magnitude to those obtained from linewidth investigations of other symmetric top molecules [13].

For a hard sphere collisional model this temperature coefficient should be -0.5. The invalidity of such a model to describe rotational relaxation may be illustrated by introducing, with reference to gas kinetic considerations, effective collision diameters b_{eff} (or cross sections πb_{eff}^2). These are related to the results from Table I and II for the pressure dependence of $1/T_2$:

$$b_{eff} = \sqrt{\delta}\sqrt[4]{\frac{RT\mu}{8\pi N_0^2}} ; \tag{6}$$

$\delta = \beta$ or γ are the pressure coefficients of $1/T_2$ for the pure gas and the mixtures, respectively, μ is the reduced molecular weight of the collision partners and N_0 Avogadro's number. The results are given in Table IV.

For colliding hard spheres, b_{eff} would be temperature independent. The large value for the pure gas indicates the long range nature of the intermolecular potential which is predominantly due to dipole-dipole interaction. The relaxation by collisions with He or H_2 is governed by higher order interaction terms, such as dipole-induced dipole and dispersion interaction, which leads to smaller values for b_{eff} in the order of the molecular nuclear frame dimension. The dipole-quadrupole interaction, absent for He, probably contributes to the larger value of b_{eff} describing collisions of CH_3CN with H_2.

Appendix

When correcting the transient emission signal of the transitions with linear Stark effect for interfering local electric fields we assume a slowly varying field with respect to the mean free path length of molecules which induces shifts $\delta\omega$ of the resonance frequency. We then may integrate Eq. (3) over the distribution function $f(\delta\omega)$ of induced shifts which

Table 4. Effective collision diameters for T_2-relaxation of $CH_3C^{15}N$ of the pure gas and mixtures with He and H_2.

Transition	Polarized M-component	T [K]	b_{eff} [Å]
CH_3CN-CH_3CN			
$J=1-2, K=\pm 1$	$M=\mp 1$	299	25.2
$J=1-2, K=\pm 1$	$M=\pm 1$	298	25.3
		273	25.4
		248	25.8
		223	26.2
$J=1-2, K=0$	$M=0$	299	26.4
$J=0-1, K=0$	$M=0$	296	28.8
		273	29.3
		247	29.5
		222	29.7
$v_8=1\left(\begin{matrix}J=1-2, K=\pm 1\\ l=\pm 1^1\end{matrix}\right)$	$M=\pm 1$	296	28.0
$v_8=1\left(\begin{matrix}J=1-2, K=\pm 1\\ l=\pm 1^2\end{matrix}\right)$	$M=\pm 1$	298	27.8
$v_8=1\left(\begin{matrix}J=1-2, K=\pm 1\\ l=\mp 1\end{matrix}\right)$	$M=\pm 1$	296	25.2
CH_3CN-He			
$J=1-2, K=\pm 1$	$M=\pm 1$	297	4.12[a]
$J=1-2, K=0$	$M=0$	297	3.89
$J=0-1, K=0$	$M=0$	293	3.99
CH_3CN-H_2			
$J=1-2, K=\pm 1$	$M=\pm 1$	295	5.14[a]
$J=1-2, K=0$	$M=0$	299	5.04
$J=0-1, K=0$	$M=0$	294	5.24

[a] Mean value from results as given in Table 2.

implies that the corresponding frequency variations are predominantly within the power and pressure broadened linewidth of the transition,

$$\overline{\Delta S(t)} = \int_{-\infty}^{+\infty} f(\delta\omega)\, A\, e^{-t/T_2} e^{-t^2/4q^2} \cdot \cos(\Delta\omega + \delta\omega)\left(t - \frac{L}{2c}\right) \mathrm{d}(\delta\omega)\,. \tag{A1}$$

For normal distribution around zero frequency shift

$$f(\delta\omega) = e^{-(\alpha\delta\omega)^2} \Big/ \int_{-\infty}^{+\infty} e^{-(\alpha\delta\omega)^2}\, \mathrm{d}(\delta\omega) \tag{A2}$$

with α a constant characterizing the width distribution, this gives

$$\overline{\Delta S(t)} = A\, e^{-t/T_2} e^{-t^2/4q^2} \cdot \frac{\int_{-\infty}^{+\infty} e^{-(\alpha\delta\omega)^2} \cos(\omega_0 - \omega + \delta\omega)\left(t - \frac{L}{2c}\right) \mathrm{d}(\delta\omega)}{\int_{-\infty}^{+\infty} e^{-(\alpha\delta\omega)^2}\, \mathrm{d}(\delta\omega)}\,. \tag{A3}$$

Integrating (A3) we have

$$\overline{\Delta S(t)} = A\, e^{-t/T_2} e^{-t^2/4q^2} \exp\left\{-\left(t - \frac{L}{2c}\right)^2 / 4\alpha^2\right\} \cdot \cos\Delta\omega\left(t - \frac{L}{2c}\right). \tag{A4}$$

For the experimental conditions ($L \cong 3$ m), $L/2c \cong 5 \cdot 10^{-9}$ sec, which allows further simplification

$$\overline{\Delta S(t)} = A e^{-t/T_2}\, e^{-t^2/4^2\tilde{q}^2} \cos\Delta\omega\left(t - \frac{L}{2c}\right) \tag{A5}$$

where $1/\tilde{q}^2 = 1/q^2 + 1/\alpha^2$.

Then, Eq. (A5) is of the form of Eq. (3) for the Doppler convoluted transient emission signal.

Acknowledgement

We thank Prof. Dr. H. Dreizler for many helpful discussions and Dr. H. D. Knauth for placing the PDP-11 computer at our disposal. The support of the Deutsche Forschungsgemeinschaft and the Fonds der Chemischen Industrie is gratefully acknowledged.

[1] R. H. Schwendeman, Ann. Rev. Phys. Chem. **29**, 537 (1978).
[2] W. E. Hoke, D. R. Bauer, and W. H. Flygare, J. Chem. Phys. **67**, 3454 (1977).
[3] J. C. McGurk, T. G. Schmalz, and W. H. Flygare, Adv. Chem. Phys. **25**, 1 (1974).
[4] H. Mäder and H. Bomsdorf, Z. Naturforsch. **33a**, 1493 (1978).
[5] C. Feuillade and J. G. Baker, J. Phys. B. Atom. Molec. Phys. **11**, 2501 (1978).
[6] J. C. McGurk, H. Mäder, R. T. Hofmann, T. G. Schmalz, and W. H. Flygare, J. Chem. Phys. **61**, 3759 (1974).
[7] H. Mäder, J. Ekkers, W. Hoke, and W. H. Flygare, J. Chem. Phys. **62**, 4380 (1975).
[8] A. Bauer, Thesis, Lille 1970.
[9] J. C. McGurk, T. G. Schmalz, and W. H. Flygare, J. Chem. Phys. **60**, 4181 (1974).
[10] I. C. Story, V. I. Metchnik, and R. W. Pearson, J. Phys. B **4**, 593 (1971).
[11] G. P. Srivastava, H. O. Gautam, and A. Kumar, J. Phys. B **6**, 743 (1973).
[12] J. A. Roberts, T. K. Tung, and C. C. Lin, J. Chem. Phys. **48**, 4046 (1968).
[13] S. C. M. Luijendijk, Thesis, Utrecht 1973.